

The impact of the local stellar radiation on the formation and evolution of dwarfs in and near Milky Way analogue

BOCHENG ZHU^{1,2} AND LIANG GAO^{2,3,1}

¹*Key Laboratory for Computational Astrophysics, National Astronomical Observatories,
Chinese Academy of Sciences, Beijing, China*

²*School of Physics and Laboratory of Zhongyuan Light, Zhengzhou university*

³*Institute for Frontiers in Astronomy and Astrophysics, Beijing Normal University, Beijing 102206, China*

ABSTRACT

We explore the effect of local stellar radiation on the formation and evolution of the dwarf galaxies near the Milk Way(MW) analogues. Using five simulations from the Auriga project, both with and without local stellar radiation, we find that the local stellar radiation, as a pre-reionization source, is quite effective to photoionize and heat the gas around the proto-MW analogues. As a result, the formation of surrounding dwarf galaxies in dark matter halos with halo masses below approximately $10^{9.5} M_{\odot}$ are significantly suppressed. After the reionization, the intensity of the local stellar radiation eventually becomes comparable to that of UVB, consequently the impact of local stellar radiation on the surrounding dwarf galaxy formation decreases with decreasing redshift, and almost vanishes after redshift $z = 4$. At present day, the bright satellite population in the simulations with and without local stellar radiation is nearly identical. While our simulation have no enough resolution to resolve the faintest satellite galaxies which are most prone to the local stellar radiation, we use accreted galaxy mass function to assess the impact, and find that the reduction in the faintest satellite is around 13 percent in case of the local stellar radiation, a factor not negligible to constrain dark matter models using the precise abundance of MW satellite galaxies.

Keywords: galaxies:dwarf – galaxies: formation – galaxies: evolution – methods: numerical – hydrodynamics

1. INTRODUCTION

Understanding the properties of dwarf galaxies provides a crucial testbed for different dark matter (DM) models, such as warm DM or fuzzy DM, which exhibit notable differences at small scale structures (Klypin et al. 1999; Bode et al. 2001; Lovell et al. 2012; Viel et al. 2013; Weinberg et al. 2015; Bullock & Boylan-Kolchin 2017; Del Popolo & Le Delliou 2017; Tulin & Yu 2018; Mocz et al. 2019; May & Springel 2021). Although the underlying cosmological model influences small scale structure, astrophysical processes like feedback re-ionisation also play significant roles (Benson et al. 2002; Okamoto et al. 2008, 2010; Sawala et al. 2016; Dashyan et al. 2018; Koudmani et al. 2021; Liu et al. 2024, etc.). For example, the well-known miss-

ing satellites problem can be possibly resolved by introducing the astrophysical processes (Benson et al. 2002). The missing satellites problem arises from the mismatch of the abundance between the prediction from N-body simulations based on the Λ CDM model and the observed satellite galaxies of the Milky Way (MW)(Klypin et al. 1999; Bullock & Boylan-Kolchin 2017). This problem can be alleviated by considering Cosmic reionization during which UV photons emitted by stars photoionize the neutral gas, heat up gas and inhabit further star formation in low mass dark matter halos(UVB, Haardt & Madau 1996; Faucher-Giguère et al. 2009; Haardt & Madau 2012; Faucher-Giguère 2020). With UVB, theoretical works using the semi-analytical model (SAM) can successfully reproduce the abundance and properties of the dwarfs (Benson et al. 2002).

Extensive studies have been carried out to explore impact of UVB on galaxy formation in low mass DM halos. For example, Okamoto et al. (2008, 2010) show

that UVB can heat up the gas to escape from the DM halo with low circular velocity, and prevent them from forming stars. [Sawala et al. \(2016\)](#) further confirms that reionization can reduce the number of dwarfs below a certain DM halo mass. [Benítez-Llambay et al. \(2017\)](#) found that the UVB can photoionize the HI gas at the outskirts of dwarfs while the HI gas at the center of dwarfs will not be affected.

Most studies discussed above assumed that reionisation process instantaneously starts and completes at redshift 6, and treated the UVB as a spatially uniform, time-dependent radiation field. However, neither the cosmic reionization is instantaneous nor the “real” UVB is uniform. The cosmic reionization is a long process, once the very first stars and galaxies form, they start to produce radiation field and thus influence galaxy formation in their surrounding DM halos. Further more the radiation field is stronger near the massive galaxies. This excess radiation may also affect the formation and evolution of the nearby dwarf galaxies.

Several studies have examined the impact of local radiation feedback on central galaxies ([Hopkins et al. 2012](#); [Roškar et al. 2014](#); [Kannan et al. 2014](#); [Ceverino et al. 2014](#); [Obreja et al. 2019](#); [Hopkins et al. 2020](#); [Zhu & Springel 2024](#), etc.). However, studies of the effect of local radiation on nearby dwarf galaxies around Milky Way-sized (MW-sized) galaxies remain scarce. [Ocvirk et al. \(2014\)](#) applied radiative transfer (RT) code to post-process simulation data from the Constrained Local Universe Simulations (CLUES; [Gottloeber et al. 2010](#)) and found that reionization for the satellites occurs from the inside-out. [Ocvirk et al. \(2016\)](#) implemented a full RT in their Cosmic Dawn (CoDa) project, which are cosmological zoom-in simulations of the Local Group. They demonstrated that local radiation substantially suppresses star formation in halos with masses below approximately $2 \times 10^9 M_{\odot}$. Further analysis by [Dawoodbhoy et al. \(2018\)](#) on the CoDa project data indicated that the star formation in halos lower than $10^9 M_{\odot}$ is suppressed by the local radiation.

In this paper, we analyze simulation data from the Auriga project using an effective RT method ([Zhu & Springel 2024](#), hereafter [Paper I](#)) to explore the impact of local stellar radiation on dwarf galaxies near proto MW-sized galaxies.

The structure of this paper is as follows. In [Section 2](#), we briefly introduce the simulation suites, the galaxy formation model and the model of the local stellar radiation implemented in the simulations. In [Section 3](#), we present and discuss our main results. Finally, we summarize our findings in [Section 4](#).

2. METHODOLOGY

2.1. The Auriga-ERT simulations

Following [Paper I](#), the simulations used in this work are based on the Auriga project, which is a suite of high-resolution magnetohydrodynamical cosmological zoom-in simulations of MW analogues ([Grand et al. 2017](#)), which has recently been made publicly available ([Grand et al. 2024](#)). The simulation is performed with AREPO code ([Springel 2010](#)), which is a N-body and moving-mesh magnetohydrodynamical code. Due to its quasi-Lagrangian nature, the AREPO code provides an adaptive resolution and manifest Galilean invariance for fluid dynamics.

Different from the original Auriga project, we incorporate the galaxy formation model from the IllustrisTNG project ([Weinberger et al. 2018](#); [Pillepich et al. 2018](#)), with star formation and stellar wind model based on ([Springel & Hernquist 2003](#)). The gas cells in the simulation convert to star-forming gas when their density exceeds a threshold and temperature is lower than a temperature criterion calculated with a two-phase ISM model. The star formation rate (SFR) is determined by this two-phase ISM model. The power of the stellar wind is then obtained based on SFR and is injected in a non-local form. The black holes (BHs) feeding and feedback model is described in [Weinberger et al. \(2018\)](#). The BHs are treated as sink particles and the BH accretion rate is calculated with the Bondi-Hoyle accretion formula. The BH feedback is separated into two modes based on the BH accretion rate. At a high accretion rate, the BH feedback is treated as a thermal mode, the feedback energy is injected isotropically in the form of thermal energy. While at a low accretion rate, the BH feedback is treated as a kinetic mode, the feedback energy is injected in the form of kinetic energy. The direction of the kinetic outflow is randomly set up in each feedback event and the kinetic energy is injected into one direction in each feedback event.

The Auriga project selected 30 MW-size halos from the EAGLE dark matter only (DMO) simulation which has a box size $100 \text{ cMpc}/h$ on a side, and re-simulated them with “zoom-in” technique ([Schaye et al. 2015](#); [Crain et al. 2015](#)). To investigate the impact of local stellar radiation on the dwarfs near main galaxies, we select 5 of 30 halos in the Auriga simulations and re-simulated them with and without the local stellar radiation described below. The IDs of five selected galaxies in the Auriga catalogue are Au3, Au6, Au16, Au5, and Au15. The simulated galaxies with local stellar radiation is referred to as StarRad simulations, while those

without the local stellar radiation is referred to as NoRad simulations.

2.2. The model of the local stellar radiation

The model of local stellar radiation used in the simulation suits is based on Kannan et al. (2014) with some modifications. The radiation field in the simulations originates from the UV background (UVB) and star forming regions, old stars and BHs of galaxies. For the UVB, we use the spectral energy distribution (SED) given by Faucher-Giguère (2020), which updates previous models to consider non-uniform shielding effects.

Radiation from star forming regions is modelled using the Binary Population and Spectral Synthesis (BPASS) v2.3 model (Eldridge et al. 2017), augmented with a power-law type emission from high mass X-ray binaries (HMXBs) and supernova remnants. For simplicity, instead of using the time-dependent SED, we use the SED of the stellar population at an age equal to 10 Myr as the radiation emitted from the young stars. We also assume that the radiation from star forming region will be absorbed when they propagate out, and the escape fraction of the radiation from the region is frequency dependent with 5% at Lyman limit frequency. Old stars and low-mass X-ray binaries are modelled similarly, with radiation properties based on a 2 Gyr old stellar population. The SED of the HMXBs and LMXBs is assumed to follow power laws, and the scaling relation between X-ray luminosity and SFR/stellar mass is obtained from Anderson et al. (2013). Note, we neglect radiation originate from BHs as the series of works focuses more on the impacts of local stellar radiation, the AGN radiation is not included in current works. Of course it should be explored in our future work.

After obtaining the SED, we then calculate the gas cooling and heating rate with radiation. For the primordial gas, the gas heating and cooling rate due to different processes is calculated by solving the ionization equilibrium equation (Katz et al. 1996). For the metal cooling and heating, the cooling and heating rate with different gas number density, temperature, redshift, the radiation flux of star forming region and old stars, and metallicity is calculated with the photoionization code CLOUDY (Ferland et al. 1998) under the ionization equilibrium assumption, and is tabulated to feed the simulations.

Once gas cooling/heating rate with radiation is obtained, we need to calculate the radiation intensity of the gas cells in simulation. For the UVB, the radiation field is assumed to be uniform. For the star forming region and old stars, we follow the treatment presented in Kannan et al. (2014) and Woods (2015). We identify star particles with a stellar age younger than 100 Myr as

young stars and the rest as old stars. Each star particle is treated as a single radiation source, and the radiation from a single star particle is scaled with the mass of the star particle. After obtaining the SED and the luminosity of all of the star particles, the radiation intensity for any gas cells is calculated by summing up the radiation irradiated by all of the star particles. Here we assume that, except for star-forming regions, the gas in a galaxy is optically thin in terms of radiation. To accelerate this calculation process, we use the octree to calculate the total radiation intensity for any gas cell. Since radiation flux from a source fade away with r^{-2} and eventually becomes weaker than the UVB, for each source we only calculate its radiation within $r = 1 \text{ cMpc}/h$.

3. RESULTS

This section explores how the local stellar radiation influences the evolution, properties, and distribution of dwarf galaxies near the simulated proto MW-sized galaxies, and compare outcomes between the NoRad and StarRad simulations. In the following discussion, we denote the “luminous halo/dwarf” as the halo/subhalo with at least one star particle.

3.1. The abundance of dwarf galaxies

In Figure 1, we present visual impression of how the local stellar radiation affect dwarf galaxies formation in our simulations. For simplicity, we only show results for the Au16 run because the galaxy is the most massive one in our simulation suite and thus is expected to make most significant impact. In the plot, luminous dwarfs are overplotted as red dots on the top of underlying DM density field of high resolution region, results for the NoRad and StarRad cases and for 4 different redshifts are shown. At a first glance, comparing the results in the NoRad and StarRad runs, the number of luminous dwarfs in the StarRad run is lower than in the NoRad run from $z = 10$ to $z = 6$. However, the discrepancy decreases with decreasing redshift. At $z = 4$, the difference between the NoRad and StarRad runs becomes negligible. These results indicate that the local stellar radiation can suppress formation of luminous halos at high redshift, and this effect becomes less pronounced with decreasing redshift. Note, near the boundary of the high resolution regions our simulations may be contaminated by low resolution particles, therefore the results near the boundary are less reliable. However, because we focus on the relative difference, this has no effect on our conclusion.

To quantify the above results, we display the time evolution of the total number of the luminous dwarfs in the high resolution regions of different simulated Auriga

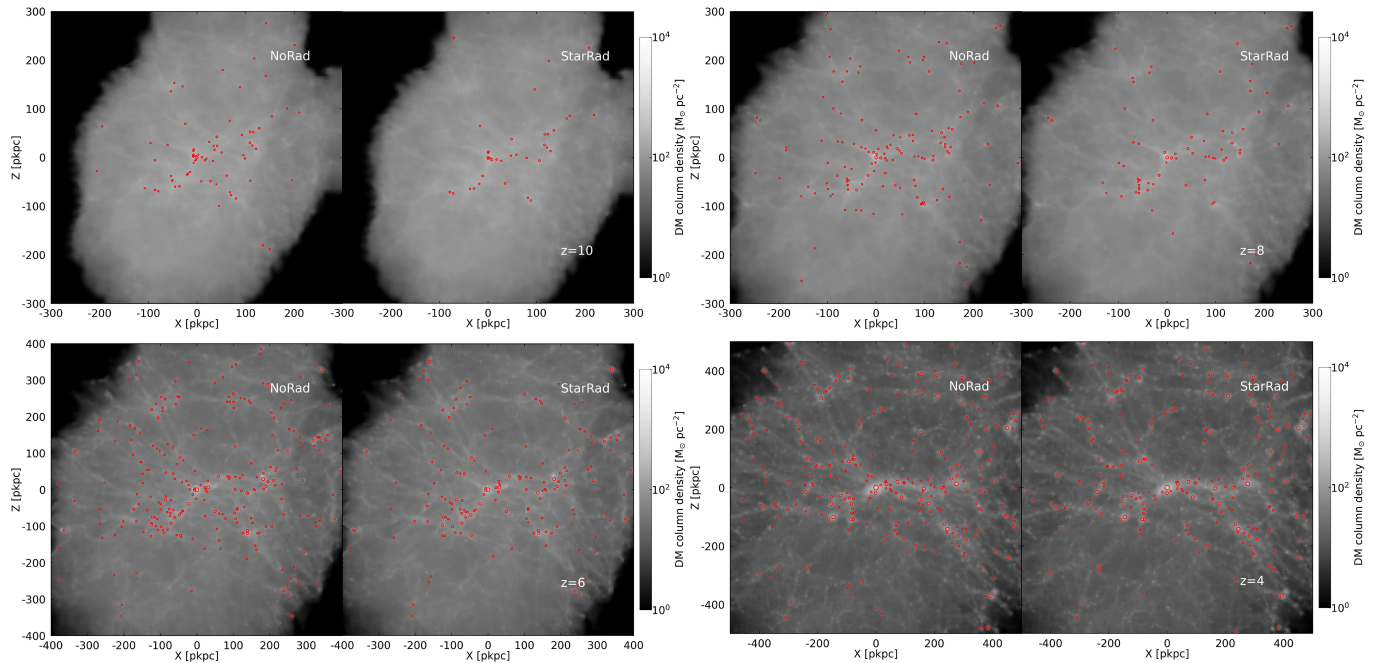


Figure 1. Dark matter density map of the Au16 simulations at $z=10, 8, 6,$ and $4,$ respectively. The red cycles indicate the luminous galaxies. In each panel, the left panel show the results of the NoRad run, while the right panel show the results in the StarRad run.

proto-galaxies in Figure 2. The sizes of the high resolution regions in different simulations are about $200 - 300$ $pkpc$ at $z = 10$ and $500 - 600$ $pkpc$ at $z=0$, below the scales the local stellar radiation are effective (optical depth of the local stellar radius equal to 3).

The relative difference of the total number between NoRad and StarRad galaxies is shown in the bottom panel of the same figure. Comparing the results in the NoRad and in StarRad runs, it is clear that the local stellar radiation makes huge impact on the formation of dwarf galaxies at high redshift. Before redshift 6, the local stellar radiation reduces the number of dwarf galaxies by half in all our runs. After redshift 6, the difference becomes eventually smaller with cosmic time and nearly vanishes at redshift after 4. The bottom panel of the same figure 2 show the time evolution of galaxy stellar mass function (GMF) from $z = 10$ to $z = 4$. At redshift $z = 10$, GMFs differ on all mass scales between the StarRad and NoRad runs, while at lower redshifts, discrepancies between the two become small and can only be seen for galaxies with a stellar mass $M_{\text{star}} \lesssim 10^7 M_{\odot}$.

Earlier works have demonstrated that the baryon processes also affect the structure formation of dark matter halos (Sawala et al. 2013; Schaller et al. 2015; Qin et al. 2017; Zheng et al. 2024). It is interesting to see how the local stellar radiation affect halo mass function (HMF). In Figure 3 we show the time evolution of HMF within 1 physical radius of the dominated halo in each simu-

lation from $z = 10$ to $z = 4$, the averaged results are shown. It is interesting that HMF in StarRad simulations is lower than in NoRad simulations for the halo mass $M_{200} \lesssim 10^{8.5} M_{\odot}$ at $z = 10$ to $z \sim 6$. This result can be explained by photoionization heating effects of the local stellar radiation, since the equilibrium temperature of the local stellar radiation ($T \sim 10^{4.5}$ K) is comparable to the virial temperature of the halos with $M_{200} \sim 10^{8.5} M_{\odot}$. At $z = 4$, the difference between the NoRad and StarRad simulations become negligible as the relative importance of the radiation decreases with redshift, which is consistent with the results shown in the Figure 1 and 2.

3.2. Gas properties

In this subsection, we investigate the impact of the local stellar radiation on the gas properties. Figure 4 presents HI column density maps of the Au13 simulations at $z=10, 8, 6,$ and $4,$ respectively. In each panel, the left one shows the results of the NoRad run, while the right one shows the result of the StarRad run. The white cycles indicate virial radius of luminous dwarfs. Clearly the HI column density of NoRad run is significantly higher than that of StarRad run before redshift 6, suggesting that the local stellar radiation can significantly reduce HI in the IGM. At redshift 4, it is hard to find difference between NoRad and StarRad run.

The above results are quantified in Figure 5, which shows the HI gas fraction of our simulations as a function

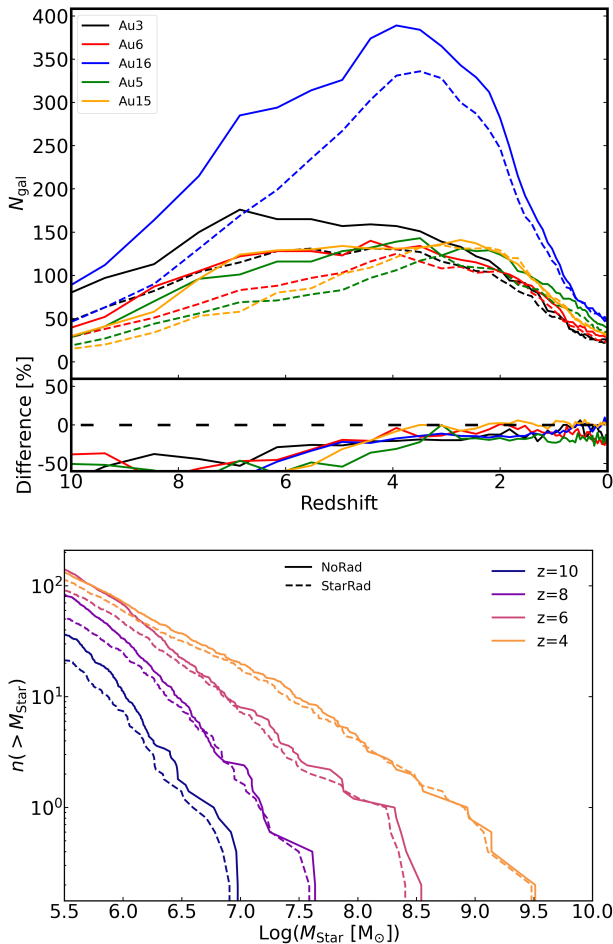


Figure 2. *Upper panel:* The time evolution of the total number of luminous dwarfs within the selected radius around the dominated galaxies. The solid lines show the results for the NoRad runs, while the dotted lines show the results for the StarRad runs. The bottom panel shows the relative difference between the NoRad and StarRad runs. *Lower panel:* The cumulative stellar mass function for the NoRad and StarRad runs at different redshifts. The solid lines show the results for the NoRad runs, while the dotted lines show the results for the StarRad runs.

of redshift. The median values of five StarRad (black) and NoStarRad (red) simulations are shown, and the shaded regions indicate scatters of different simulation sets. By construction, the gas is completely neutral in the NoRad runs at $z \gtrsim 6$. However, the gas in the StarRad runs are partly ionized at $z \gtrsim 6$, while the HI fractions varies significantly among different runs due to different dominated stellar radiation sources. After redshift about 6, the neutral fraction in both simulation sets become closer.

A well-known effect of photoionization is that it can heat up gas to escape from low mass DM halos, leading to a significant reduction in the gas fraction, as shown

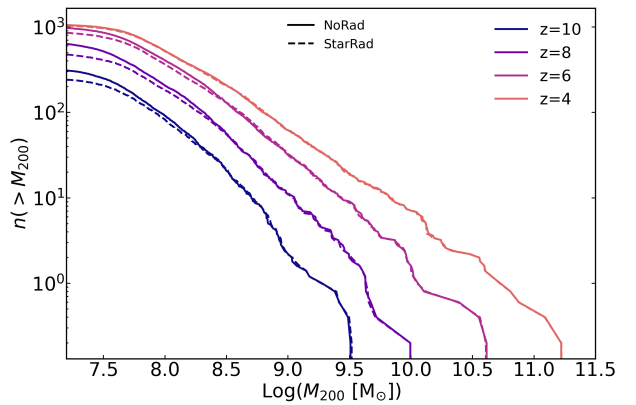


Figure 3. The cumulative halo mass function for the NoRad and StarRad simulations. The solid lines show the results for the NoRad runs, while the dotted lines show the results for the StarRad runs.

by a few previous studies in context of the cosmic reionization (Barkana & Loeb 2000; Gnedin 2000; Okamoto et al. 2008; Wise & Abel 2008). The same physics should of course apply to the local stellar radiation. In Figure 6 we present the time evolution of the baryon fraction of dark matter halo as a function of halo mass in different runs, results for 4 different redshifts are shown. For dark matter halos with a halo mass $M_{\star} \lesssim 10^{9.5} \text{M}_{\odot}$, the baryon fraction is quite different between the “NoRad” and “StarRad” runs, the difference vanishes for the halos with higher masses. In addition, the difference decrease with decreasing redshift, indicating the effects of the local stellar radiation for suppressing the gas accretion of the low-mass halo become weaker with decreasing redshift, which have similar trends as the results discussed above.

The impact of the uniform UVB on gas properties in low mass dark matter halos is well understood. To evaluate the impact of the local stellar radiation, it is interesting to compare its intensity to that of UVB. In Figure 7, we present the gas mass distribution of the ratio between radiation from star forming region and UVB at various redshift, the results averaged from five StarRad simulations are shown. Based on the cooling/heating rate shown in Zhu & Springel (2024), only the gas cell with temperature lower than $\sim 10^{4.5} \text{K}$ will be significantly affected by the radiation, thus only the gas cell with the temperature lower than $10^{4.5} \text{K}$ is included in this figure. In the figure, we can see that before $z = 8$ the intensity of the local radiation J_{YS} (since the local radiation is dominated by young stellar region, we only take this part into account) is significantly higher than that of UVB (J_{UVB}) in the simulation. After $z = 6$, the peak of the ratio distribution is close to unit, indicating that after the epoch of reionization (at $z \sim 5.5$), the lo-

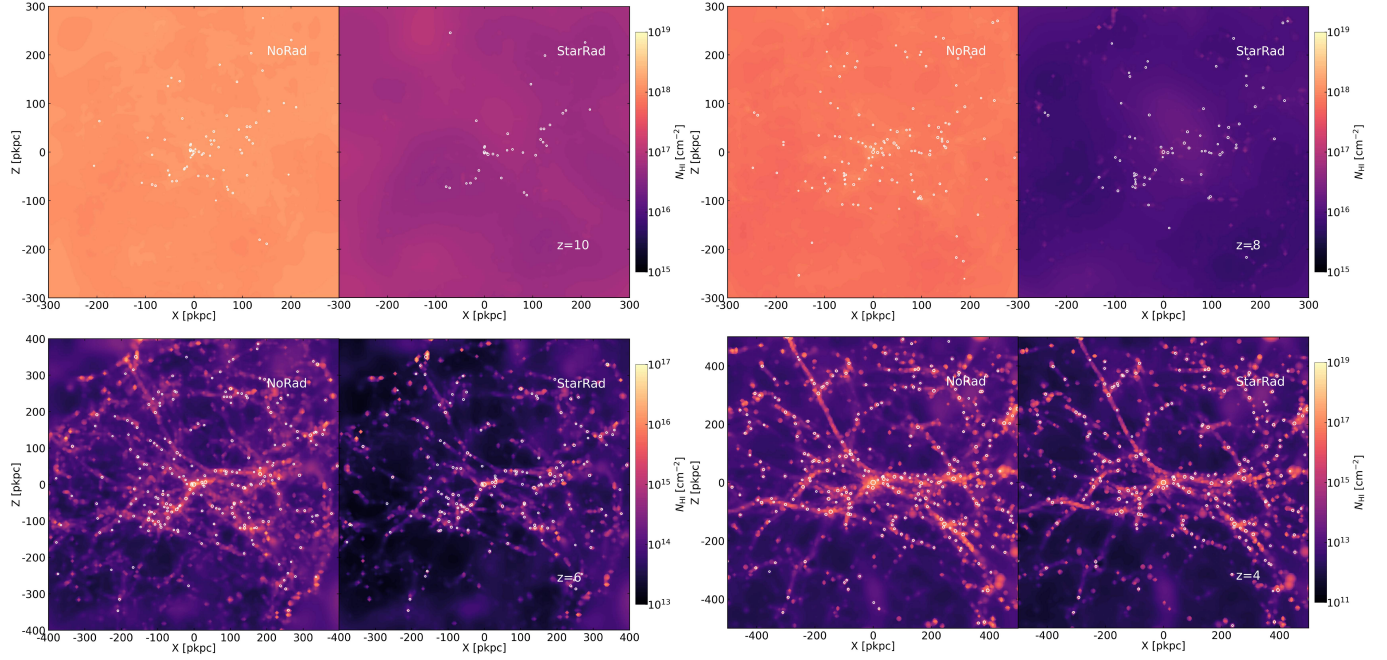


Figure 4. Similar to the Figure 1, but for HI column density gas at different redshifts in the Au13 NoRad and StarRad simulations. The white circles indicate luminous galaxies.

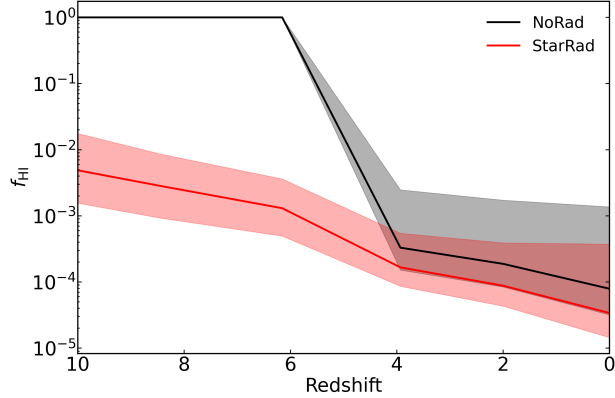


Figure 5. The median values of HI gas fraction within a range of the selected radius around each main halo as a function of redshift. The shaded region represent 10% and 90% of the values in each simulation set.

cal stellar radiation and UVB becomes comparable. The effects of the local stellar radiation become weak since its effects are only equivalent to approximately doubling UVB enhancement and the fraction of the cold gas become lower and lower after the epoch of reionization.

3.3. The abundance of satellites at $z=0$

In this subsection, we explore how the local stellar radiation affect the satellite population at the present day. In Figure 8, we compare the V-band luminosity function of the satellites in the StarRad and NoRad runs, the averaged values in each simulation sets are shown. For reference, we also show observational result from

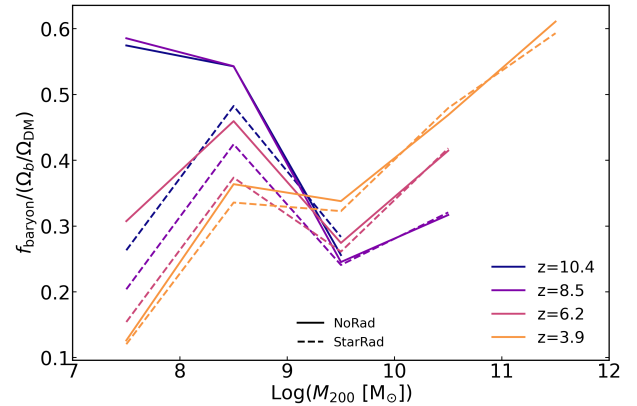


Figure 6. The median baryon fraction of dark matter halos as a function of halo mass at various redshifts.

Newton et al. (2018). Clearly, limited by numerical resolution, both simulation sets can only resolve classical satellites, which agree almost perfectly with each other in both simulation sets, suggesting the local stellar radiation make little effect on the brighter satellite galaxy population. This might not be surprising as the local stellar radiation only affects galaxy formation in low mass halos at high z , the brighter satellites are less affected by the local stellar radiation.

While it is expected that local stellar radiation only affect the faint end of satellite luminosity function, our simulations lack the necessary resolution to address this problem directly. However, still we can get some hints by looking at the accreted dwarf galaxies at infall, which are

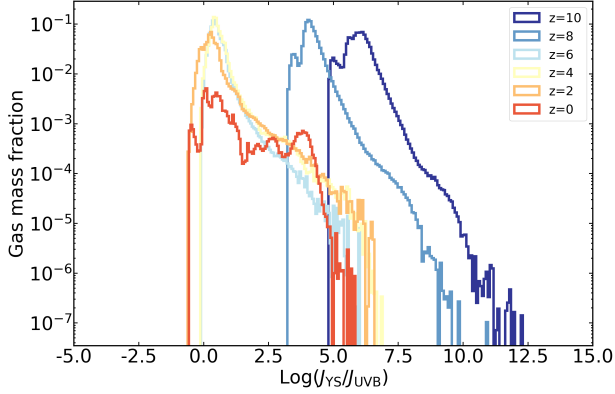


Figure 7. The gas mass distribution of the ratio between the intensity of the local stellar radiation and UVB within a range of the selected radius around the main halos at different redshifts. The gas is selected by the criterion that the temperature is lower than $10^{4.5}$ K.

possible progenitors of satellite galaxies at the present day. Once they were accreted to the central halos, some of the progenitors are physically disrupted by tidal effects, while some of them may disappear only due to numerical resolution. Our simulations have enough resolution to resolve all luminosity dwarf galaxies before infall, and hence we still can assess the impact of the local stellar radiation on the final satellite galaxy population according to these progenitors. In Figure 9, we show the progenitor mass function in the NoRad and StarRad runs. Here a progenitor is defined as a galaxy accreted into the virial radius of the main halo, the stellar mass at the accretion time is recorded as the mass of progenitors. Again, the averaged values are shown for both simulation sets. Apparently, both simulations agree very well on the relatively massive progenitors $M \gtrsim 10^8 M_\odot$. Below this mass, two runs deviates, at the smallest mass scale two sets runs differ by 13%, implying the local stellar radiation can make a difference in the satellite population at the same level. While the difference is not large, it should be take into account when using the abundance of MW satellite galaxies to constrain the dark matter models (Kennedy et al. 2014; Bose et al. 2016; Nadler et al. 2021; Newton et al. 2021; Hayashi et al. 2021; Dekker et al. 2022).

4. SUMMARY AND CONCLUSION

In this work, we explore the impact of the local stellar radiation on the formation and evolution of the dwarf galaxies in the surrounding of the MW-analogues by using the simulations from Paper I. Our main findings can be summarized as follows.

The local stellar radiation as a ionizing source can photoionize and heat up the IGM in the vicinity of proto-MW analogues before the reionization. Conse-

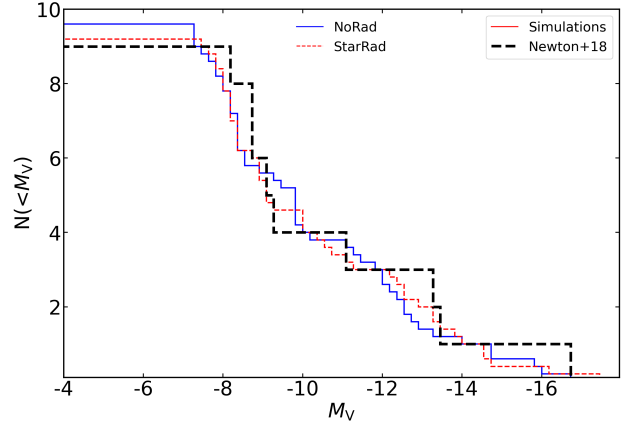


Figure 8. The V-band luminosity function of satellite galaxies in the main halos at $z = 0$. The thick dashed line represents the observational results from Newton et al. (2018).

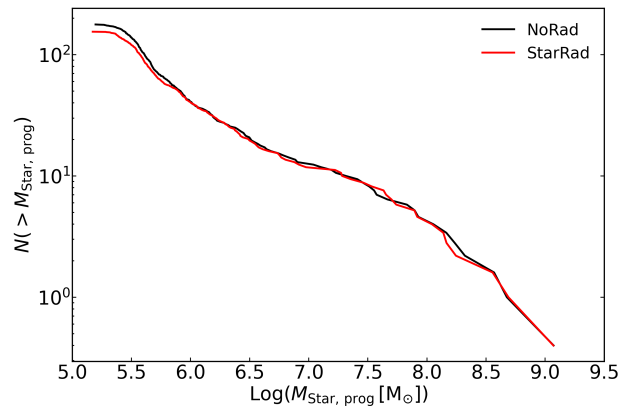


Figure 9. The accreted galaxy stellar mass function over the entire halo assembly.

quently, the neutral gas fraction in the volume with local stellar radiation is significantly reduced before the reionization. The intensity of the local stellar radiation is stronger than that of UVB by large factors before $z = 6$, while they become comparable afterwards.

Due to photoionization by the local stellar radiation, the low mass DM halos in proto-MW region are less efficient to capture gas to form stars, as a result the abundance of dwarf galaxy is significantly suppressed before reionization. The total amount of the dwarfs around the dominant galaxy is suppressed in the StarRad galaxies at $z \gtrsim 6$ by a factor of about half. However, after $z \sim 6$, when the reionization complete, the difference in the total amount of dwarf galaxies between the simulations with and without the local stellar radiation decreases with decreasing redshift, which is less than 10% at $z \lesssim 3$.

Although the impact of local stellar radiation on the formation of dwarf galaxies are large at high redshift, this does not propagate to the present day. The V-band

luminosity function of the resolved satellites in the halos of the simulations with and without the local stellar radiation is almost exactly the same. We further compare the accreted galaxy stellar mass function in both simulation sets, and find the the local radiation can reduce the abundance of the faintest satellite by a factor of 13 percent.

It is worth noting that there are still some limitations in the current treatment of the models of local stellar radiation. Since the treatment of the radiation transfer bases on optically-thin assumption, which means that such treatment will overestimate the effects of radiation, thus the results presented above are only an upper limit

of impacts of the local stellar radiation. These motivate us to implement a more accurate radiation transfer in our future work.

We thank Shi Shao and Lizhi Xie for helpful discussions. The authors thank Volker Springel for providing the data. We acknowledge the supports from the National Natural Science Foundation of China (Grant No. 11988101) and the K. C. Wong Education Foundation. Data analysis were performed on the Freya compute cluster of MPA, operated by the Max Planck Computing and Data Facility.

REFERENCES

- Anderson, M. E., Bregman, J. N., & Dai, X. 2013, *ApJ*, 762, 106, doi: [10.1088/0004-637X/762/2/106](https://doi.org/10.1088/0004-637X/762/2/106)
- Barkana, R., & Loeb, A. 2000, *ApJ*, 531, 613, doi: [10.1086/308503](https://doi.org/10.1086/308503)
- Benítez-Llambay, A., Navarro, J. F., Frenk, C. S., et al. 2017, *MNRAS*, 465, 3913, doi: [10.1093/mnras/stw2982](https://doi.org/10.1093/mnras/stw2982)
- Benson, A. J., Frenk, C. S., Lacey, C. G., Baugh, C. M., & Cole, S. 2002, *MNRAS*, 333, 177, doi: [10.1046/j.1365-8711.2002.05388.x](https://doi.org/10.1046/j.1365-8711.2002.05388.x)
- Bode, P., Ostriker, J. P., & Turok, N. 2001, *ApJ*, 556, 93, doi: [10.1086/321541](https://doi.org/10.1086/321541)
- Bose, S., Hellwing, W. A., Frenk, C. S., et al. 2016, *MNRAS*, 455, 318, doi: [10.1093/mnras/stv2294](https://doi.org/10.1093/mnras/stv2294)
- Bullock, J. S., & Boylan-Kolchin, M. 2017, *ARA&A*, 55, 343, doi: [10.1146/annurev-astro-091916-055313](https://doi.org/10.1146/annurev-astro-091916-055313)
- Ceverino, D., Klypin, A., Klimek, E. S., et al. 2014, *MNRAS*, 442, 1545, doi: [10.1093/mnras/stu956](https://doi.org/10.1093/mnras/stu956)
- Crain, R. A., Schaye, J., Bower, R. G., et al. 2015, *MNRAS*, 450, 1937, doi: [10.1093/mnras/stv725](https://doi.org/10.1093/mnras/stv725)
- Dashyan, G., Silk, J., Mamon, G. A., Dubois, Y., & Hartwig, T. 2018, *MNRAS*, 473, 5698, doi: [10.1093/mnras/stx2716](https://doi.org/10.1093/mnras/stx2716)
- Dawoodbhoy, T., Shapiro, P. R., Ocvirk, P., et al. 2018, *MNRAS*, 480, 1740, doi: [10.1093/mnras/sty1945](https://doi.org/10.1093/mnras/sty1945)
- Dekker, A., Ando, S., Correa, C. A., & Ng, K. C. Y. 2022, *PhRvD*, 106, 123026, doi: [10.1103/PhysRevD.106.123026](https://doi.org/10.1103/PhysRevD.106.123026)
- Del Popolo, A., & Le Delliou, M. 2017, *Galaxies*, 5, 17, doi: [10.3390/galaxies5010017](https://doi.org/10.3390/galaxies5010017)
- Eldridge, J. J., Stanway, E. R., Xiao, L., et al. 2017, *PASA*, 34, e058, doi: [10.1017/pasa.2017.51](https://doi.org/10.1017/pasa.2017.51)
- Faucher-Giguère, C.-A. 2020, *MNRAS*, 493, 1614, doi: [10.1093/mnras/staa302](https://doi.org/10.1093/mnras/staa302)
- Faucher-Giguère, C.-A., Lidz, A., Zaldarriaga, M., & Hernquist, L. 2009, *ApJ*, 703, 1416, doi: [10.1088/0004-637X/703/2/1416](https://doi.org/10.1088/0004-637X/703/2/1416)
- Ferland, G. J., Korista, K. T., Verner, D. A., et al. 1998, *PASP*, 110, 761, doi: [10.1086/316190](https://doi.org/10.1086/316190)
- Gnedin, N. Y. 2000, *ApJ*, 542, 535, doi: [10.1086/317042](https://doi.org/10.1086/317042)
- Gottloeber, S., Hoffman, Y., & Yepes, G. 2010, arXiv e-prints, arXiv:1005.2687, doi: [10.48550/arXiv.1005.2687](https://doi.org/10.48550/arXiv.1005.2687)
- Grand, R. J. J., Fragkoudi, F., Gómez, F. A., et al. 2024, arXiv e-prints, arXiv:2401.08750, doi: [10.48550/arXiv.2401.08750](https://doi.org/10.48550/arXiv.2401.08750)
- Grand, R. J. J., Gómez, F. A., Marinacci, F., et al. 2017, *MNRAS*, 467, 179, doi: [10.1093/mnras/stx071](https://doi.org/10.1093/mnras/stx071)
- Haardt, F., & Madau, P. 1996, *ApJ*, 461, 20, doi: [10.1086/177035](https://doi.org/10.1086/177035)
- . 2012, *ApJ*, 746, 125, doi: [10.1088/0004-637X/746/2/125](https://doi.org/10.1088/0004-637X/746/2/125)
- Hayashi, K., Ferreira, E. G. M., & Chan, H. Y. J. 2021, *ApJL*, 912, L3, doi: [10.3847/2041-8213/abf501](https://doi.org/10.3847/2041-8213/abf501)
- Hopkins, P. F., Grudić, M. Y., Wetzel, A., et al. 2020, *MNRAS*, 491, 3702, doi: [10.1093/mnras/stz3129](https://doi.org/10.1093/mnras/stz3129)
- Hopkins, P. F., Quataert, E., & Murray, N. 2012, *MNRAS*, 421, 3522, doi: [10.1111/j.1365-2966.2012.20593.x](https://doi.org/10.1111/j.1365-2966.2012.20593.x)
- Kannan, R., Stinson, G. S., Macciò, A. V., et al. 2014, *MNRAS*, 437, 2882, doi: [10.1093/mnras/stt2098](https://doi.org/10.1093/mnras/stt2098)
- Katz, N., Weinberg, D. H., & Hernquist, L. 1996, *ApJS*, 105, 19, doi: [10.1086/192305](https://doi.org/10.1086/192305)
- Kennedy, R., Frenk, C., Cole, S., & Benson, A. 2014, *MNRAS*, 442, 2487, doi: [10.1093/mnras/stu719](https://doi.org/10.1093/mnras/stu719)
- Klypin, A., Kravtsov, A. V., Valenzuela, O., & Prada, F. 1999, *ApJ*, 522, 82, doi: [10.1086/307643](https://doi.org/10.1086/307643)
- Koudmani, S., Henden, N. A., & Sijacki, D. 2021, *MNRAS*, 503, 3568, doi: [10.1093/mnras/stab677](https://doi.org/10.1093/mnras/stab677)
- Liu, W., Veilleux, S., Canalizo, G., et al. 2024, *ApJ*, 965, 152, doi: [10.3847/1538-4357/ad2b63](https://doi.org/10.3847/1538-4357/ad2b63)
- Lovell, M. R., Eke, V., Frenk, C. S., et al. 2012, *MNRAS*, 420, 2318, doi: [10.1111/j.1365-2966.2011.20200.x](https://doi.org/10.1111/j.1365-2966.2011.20200.x)
- May, S., & Springel, V. 2021, *MNRAS*, 506, 2603, doi: [10.1093/mnras/stab1764](https://doi.org/10.1093/mnras/stab1764)

- Mocz, P., Fialkov, A., Vogelsberger, M., et al. 2019, *Phys. Rev. Lett.*, 123, 141301, doi: [10.1103/PhysRevLett.123.141301](https://doi.org/10.1103/PhysRevLett.123.141301)
- Nadler, E. O., Drlica-Wagner, A., Bechtol, K., et al. 2021, *PhRvL*, 126, 091101, doi: [10.1103/PhysRevLett.126.091101](https://doi.org/10.1103/PhysRevLett.126.091101)
- Newton, O., Cautun, M., Jenkins, A., Frenk, C. S., & Helly, J. C. 2018, *MNRAS*, 479, 2853, doi: [10.1093/mnras/sty1085](https://doi.org/10.1093/mnras/sty1085)
- Newton, O., Leo, M., Cautun, M., et al. 2021, *JCAP*, 2021, 062, doi: [10.1088/1475-7516/2021/08/062](https://doi.org/10.1088/1475-7516/2021/08/062)
- Obreja, A., Macciò, A. V., Moster, B., et al. 2019, *MNRAS*, 490, 1518, doi: [10.1093/mnras/stz2639](https://doi.org/10.1093/mnras/stz2639)
- Ocvirk, P., Gillet, N., Aubert, D., et al. 2014, *ApJ*, 794, 20, doi: [10.1088/0004-637X/794/1/20](https://doi.org/10.1088/0004-637X/794/1/20)
- Ocvirk, P., Gillet, N., Shapiro, P. R., et al. 2016, *MNRAS*, 463, 1462, doi: [10.1093/mnras/stw2036](https://doi.org/10.1093/mnras/stw2036)
- Okamoto, T., Frenk, C. S., Jenkins, A., & Theuns, T. 2010, *MNRAS*, 406, 208, doi: [10.1111/j.1365-2966.2010.16690.x](https://doi.org/10.1111/j.1365-2966.2010.16690.x)
- Okamoto, T., Gao, L., & Theuns, T. 2008, *MNRAS*, 390, 920, doi: [10.1111/j.1365-2966.2008.13830.x](https://doi.org/10.1111/j.1365-2966.2008.13830.x)
- Pillepich, A., Springel, V., Nelson, D., et al. 2018, *MNRAS*, 473, 4077, doi: [10.1093/mnras/stx2656](https://doi.org/10.1093/mnras/stx2656)
- Qin, Y., Duffy, A. R., Mutch, S. J., et al. 2017, *MNRAS*, 467, 1678, doi: [10.1093/mnras/stx083](https://doi.org/10.1093/mnras/stx083)
- Roškar, R., Teyssier, R., Agertz, O., Wetzstein, M., & Moore, B. 2014, *MNRAS*, 444, 2837, doi: [10.1093/mnras/stu1548](https://doi.org/10.1093/mnras/stu1548)
- Sawala, T., Frenk, C. S., Crain, R. A., et al. 2013, *MNRAS*, 431, 1366, doi: [10.1093/mnras/stt259](https://doi.org/10.1093/mnras/stt259)
- Sawala, T., Frenk, C. S., Fattahi, A., et al. 2016, *MNRAS*, 456, 85, doi: [10.1093/mnras/stv2597](https://doi.org/10.1093/mnras/stv2597)
- Schaller, M., Frenk, C. S., Bower, R. G., et al. 2015, *MNRAS*, 451, 1247, doi: [10.1093/mnras/stv1067](https://doi.org/10.1093/mnras/stv1067)
- Schaye, J., Crain, R. A., Bower, R. G., et al. 2015, *MNRAS*, 446, 521, doi: [10.1093/mnras/stu2058](https://doi.org/10.1093/mnras/stu2058)
- Springel, V. 2010, *MNRAS*, 401, 791, doi: [10.1111/j.1365-2966.2009.15715.x](https://doi.org/10.1111/j.1365-2966.2009.15715.x)
- Springel, V., & Hernquist, L. 2003, *MNRAS*, 339, 289, doi: [10.1046/j.1365-8711.2003.06206.x](https://doi.org/10.1046/j.1365-8711.2003.06206.x)
- Tulin, S., & Yu, H.-B. 2018, *PhR*, 730, 1, doi: [10.1016/j.physrep.2017.11.004](https://doi.org/10.1016/j.physrep.2017.11.004)
- Viel, M., Becker, G. D., Bolton, J. S., & Haehnelt, M. G. 2013, *PhRvD*, 88, 043502, doi: [10.1103/PhysRevD.88.043502](https://doi.org/10.1103/PhysRevD.88.043502)
- Weinberg, D. H., Bullock, J. S., Governato, F., Kuzio de Naray, R., & Peter, A. H. G. 2015, *Proceedings of the National Academy of Science*, 112, 12249, doi: [10.1073/pnas.1308716112](https://doi.org/10.1073/pnas.1308716112)
- Weinberger, R., Springel, V., Pakmor, R., et al. 2018, *MNRAS*, 479, 4056, doi: [10.1093/mnras/sty1733](https://doi.org/10.1093/mnras/sty1733)
- Wise, J. H., & Abel, T. 2008, *ApJ*, 685, 40, doi: [10.1086/590417](https://doi.org/10.1086/590417)
- Woods, R. 2015, PhD thesis, McMaster University, Canada
- Zheng, H., Bose, S., Frenk, C. S., et al. 2024, *arXiv e-prints*, arXiv:2403.17044, doi: [10.48550/arXiv.2403.17044](https://doi.org/10.48550/arXiv.2403.17044)
- Zhu, B., & Springel, V. 2024, *MNRAS*, 533, 4360, doi: [10.1093/mnras/stae2047](https://doi.org/10.1093/mnras/stae2047)